Phase Behavior of Polystyrene-*block*-Poly(*n*-butyl-*ran*-*n*-hexyl) Methacrylate Copolymers

Hong Chul Moon, Sung Hyun Han, and Jin Kon Kim*

National Creative Research Initiative Center for Block Copolymer Self-Assembly, Department of Chemical Engineering, Pohang University of Science and Technology, Pohang, Kyungbuk 790-784, Republic of Korea

Guang Hua Li

School of Chemistry & Chemical Engineering, Guangxi University, No. 100 Daxue Road, Nanning, Guangxi 530-004, China

Junhan Cho*

Department of Polymer Science and Engineering, and Center for Photofunctional Energy Materials, Dankook University, Hyperstructured Organic Materials Research Center, Yongin-si, Gyeonggi-do 448-701, Korea

Received March 23, 2008; Revised Manuscript Received July 2, 2008

ABSTRACT: The phase behavior of symmetric polystyrene-*block*-poly(*n*-butyl-*ran*-*n*-hexyl) methacrylate copolymers (PS-*b*-Pn(B-*r*-H)MA) with various molecular weights was investigated by small-angle X-ray scattering (SAXS), rheometry, polarized optical microscopy (POM), and static birefringence. PS-*b*-PnBMA exhibited a lower disorder-to-order transition (LDOT), whereas PS-*b*-PnHMA exhibited an order-to-disorder transition (UODT). However, when a random copolymer of Pn(B-*r*-H)MA was used as one of the blocks, PS-*b*-Pn(B-*r*-H)MA showed closed-loop phase behavior having both LDOT and UODT, which was seen in PS-*b*-poly(*n*-pentyl methacrylate) copolymer, when the total molecular weight was judiciously controlled. The phase behavior change by including a random copolymer was explained by an argument based on a compressible random phase approximation. We also found that the pressure coefficient of both transition temperatures of PS-*b*-Pn(B-*r*-H)MA was much larger than that of neat PS-*b*-PnBMA and PS-*b*-PnHMA.

1. Introduction

The phase behavior of block copolymers has been intensively investigated experimentally and theoretically due to their self-assembly to form lamellae, hexagonally packed cylinders, spheres (body-centered cubic), and gyroids.[1−5] It depends on the volume fraction (f) of one of blocks, the degree of polymerization (N), and the Flory−Huggins segmental interaction parameter (χ).[1] Upon heating, most block copolymers exhibit order-to-disorder transition (ODT) of enthalpic origin,[1−5] whereas some block copolymers, for example polystyrene-*block*-poly(*n*-butyl methacrylate) (PS-*b*-PnBMA),[6] show lower disorder-to-order transition (LDOT). We reported that polystyrene-*block*-poly(*n*-pentyl methacrylate) (PS-*b*-PnPMA) shows both LDOT and upper order-to-disorder transition (UODT) which form the closed loop.[7−14] The LDOT, which is of entropic origin, can be driven when resolving entropic loss either in forming directional interaction pairs between dissimilar components or in mixing components with different pendent group structures or compressibilities.[15−20] At higher temperatures, the translational (or combinatorial) entropic contribution can in principle overcome the free energy in the ordered state to yield disorder. The closed-loop phase behavior for weakly interacting PS-*b*-PnPMA originates in directional interaction, the dipole/induced dipole interaction from the phenyl ring in PS and the polar ester group of PnPMA,[21,22] and the interplay between such interaction and combinatorial entropy.[20] Furthermore, PS-*b*-PnPMA having disparity in their compressibilities exhibited very large pressure coefficients (dT/dP) of LDOT (+725 °C/kbar) and UODT(−725 °C/kbar).[10]

Phase behavior of polystyrene-*block*-poly(*n*-alkyl methacrylate) copolymers was significantly changed when a random copolymer having different alkyl chains was used as one of the blocks. Ruzette et al. found that polystyrene-*block*-poly(methacrylate-*ran*-lauryl methacrylate) copolymer (PS-*b*-P(MMA-*r*-LMA)) exhibited the LDOT,[23] even though both PS-*b*-PMMA and PS-*b*-PLMA exhibited the ODT.[23,24] They explained this interesting phase behavior by the fact that the specific volume and the solubility parameter of P(MMA-*r*-LMA) are very similar to those of neat PnBMA,[23,24] which exhibits the LDOT. They also found that the dT/dP of the LDOT of PS-*b*-P(MMA-*r*-LMA) was 150 °C/kbar,[24] which is similar to that (147 °C/kbar) of PS-*b*-PnBMA.[25]

If this scenario works, polystyrene-*block*-poly(*n*-butyl methacrylate-*ran*-*n*-hexyl methacrylate) copolymers (PS-*b*-Pn(B-*r*-H)MA) might show a closed-loop phase behavior similar to PS-*b*-PnPMA, even though PS-*b*-PnHMA showed only an order-to-disorder transition, whereas PS-*b*-PnBMA exhibited LDOT type phase behavior.[23−26]

In this study, we investigated the phase behavior of PS-*b*-Pn(B-*r*-H)MA with various molecular weights prepared by sequential anionic polymerization by small-angle X-ray scattering (SAXS), rheometry, polarized optical microscopy (POM), and static birefringence. When the total molecular weight was judiciously controlled, we observed that PS-*b*-Pn(B-*r*-H)MA exhibited the closed-loop phase behavior having both LDOT and UODT within an experimentally accessible temperature range. We found that to observe the closed-loop phase behavior PS-*b*-Pn(B-*r*-H)MA the total molecular weight should be very similar to PS-*b*-PnPMA. The pressure coefficient of the transi-

* To whom correspondence should be addressed. E-mail: jkkim@postech.ac.kr; jhcho@dankook.ac.kr.

10.1021/ma800645u CCC: $40.75
Published on Web 08/21/2008

Table 1. Molecular Characteristics of Polymers Employed in This Study

sample code	M_n	M_w/M_n	w_{PS}	PS-*b*-Pn(B-*r*-H)MA-L/ PS-*b*-Pn(B-*r*-H)MA-H (w/w)	transition type
PS-*b*-Pn(B-*r*-H)MA-L	40 700	1.05	0.52	100/0	fully disordered
PS-*b*-Pn(B-*r*-H)MA-B1	48 400[a]			25/75	closed loop
PS-*b*-Pn(B-*r*-H)MA-B2	48 800[a]			22/78	closed loop
PS-*b*-Pn(B-*r*-H)MA-B3	49 000[a]			20/80	closed loop
PS-*b*-Pn(B-*r*-H)MA-B4	49 200[a]			18.6/81.4	closed loop
PS-*b*-Pn(B-*r*-H)MA-B5	49 400[a]			17.5/82.5	closed loop
PS-*b*-Pn(B-*r*-H)MA-H	51 700	1.07	0.52	0/100	fully ordered
PnBMA	95 400	1.04			
PnHMA	148 000	1.04			
PnPMA	105 700	1.04			
Pn(B-*r*-H)MA	173 000	1.04		52 (PnBMA wt %)	

[a] Calculated by $(M_n)_{blend} = [(w_1/M_{n,1}) + (w_2/M_{n,2})]^{-1}$, where w_i and $M_{n,i}$ are weight fractions and number-average molecular weight of polymer i, respectively.

tion temperatures was much larger than that for neat PS-*b*-PnBMA and PS-*b*-PnHMA.

2. Experimental Section

Materials and Characterization. PS-*b*-Pn(B-*r*-H)MA copolymers with various molecular weights were synthesized by sequential anionic polymerization of styrene and the mixture composed of an equal amount of *n*-butyl methacrylate (*n*-BMA) and *n*-hexyl methacrylate (*n*-HMA) in dried tetrahydrofuran (THF) at −78 °C under a purified argon atmosphere with *sec*-butyllithium (*sec*-BuLi) and dried LiCl. The dibutylmagnesium was used to purify styrene monomer, and the trioctylaluminum was used to purify *n*-BMA and *n*-HMA. After the polymerization of styrene for 1 h, a mixture of *n*-BMA and *n*-HMA was dropwise added into the reactor and reacted for 7 h. We also synthesized anionically PnBMA, PnHMA, and PnPMA homopolymers and Pn(B-*r*-H)MA copolymer. The weight- and number-average molecular weights, M_w and M_n, respectively, were measured by size exclusion chromatography (SEC: Waters) with PS standards in tetrahydrofuran (THF) solution, and the weight fraction of the PS block was determined by ^{1}H nuclear magnetic resonance spectroscopy (NMR: Bruker DPX300). The molecular characteristics of the synthesized PS-*b*-Pn(B-*r*-H)MA, PnBMA, PnHMA, PnPMA, and Pn(B-*r*-H)MA are summarized in Table 1. Since the phase behavior and the transition temperatures are so sensitive to a small change in the total molecular weight, we carefully mixed higher molecular weight and lower molecular weight PS-*b*-Pn(B-*r*-H)MAs to have five additional molecular weights. The blend of two block copolymers was prepared by using methylene chloride as a solvent and slowly evaporating solvent for 24 h at room temperature. All samples were annealed at 140 °C for 48 h under vacuum.

Depolarized Transmitted Light. Depolarized transmitted light scattering[27,28] was used to determine the transition temperatures (LDOT and UODT) of PS-*b*-Pn(B-*r*-H)MAs with various molecular weights. Vertically polarized light from a HeNe laser with a wavelength of 632.8 nm passed through the sample and a horizontal analyzing polarizer onto a photodetector. Samples with thickness of 1.0 mm and a diameter of 5 mm were covered by two glass disks, and then the depolarized light intensity was measured at a heating rate of 1 °C/min.

Rheological Properties. An Advanced Rheometric Expansion System (TI Instruments) with parallel plates of 25 mm diameter was used to perform dynamic temperature sweep of storage and loss moduli (G' and G'') under isochronal conditions upon heating at a rate of 0.5 °C/min. The angular frequency and the strain amplitude were 0.1 rad/s and 0.05, respectively, which lie in the linear viscoelasticity range.

Small-Angle X-ray Scattering (SAXS). SAXS experiments were performed on beamlines 4C1 and 4C2 at the Pohang Light Source (Korea), where a W/B4C double multilayer delivered monochromatic X-rays on the samples with a wavelength of 0.1608 nm.[29] A 2-D CCD camera (Princeton Instruments, SCX-TE/CCD-1242) was used to collect the scattered X-rays. The sample thickness was 1.0 mm, and the exposure time was 90 s.

Differential Scanning Calorimetry (DSC). To measure the glass transition temperature (T_g) of PnBMA and PnHMA homopolymers and Pn(B-*r*-H)MA, DSC thermograms (Seiko instruments: model DSC-220CU) were obtained upon heating at a rate of 20 °C/min from −50 to 150 °C. The thermogram was calibrated by tin and indium.

Temperature Dependence of Specific Volume. Temperature dependences of specific volume for PnBMA, PnHMA, PnPMA homopolymers, and Pn(B-*r*-H)MA were measured. For this experiment, thin films of each polymer with a thickness of ∼140 nm were prepared by spin-coating from 1-butanol solution and annealed at 120 °C under vacuum for 24 h. The specific volumes of each polymer were determined from the measurements of changes in film thickness by spectroscopic ellipsometry (J.A. Woollam) at an incidence angle of 75°. The density of each polymer measured with a density meter (Mettler Toledo) at 30 °C was 1.031, 0.998, 1.007, and 1.009 g/cm^3 for PnBMA, PnHMA, PnPMA, and Pn(B-*r*-H)MA, respectively. Because of the very small thickness of the film compared with the surface area of the film, the change in film thickness ($\Delta H/H_0$) was assumed to be the same as the change in volume ($\Delta V/V_0$) with increasing temperature, where H_0 and V_0 are the thickness and the volume of the film at 30 °C.

3. Results and Discussion

Figures 1a,b are GPC chromatograms for PS-*b*-Pn(B-*r*-H)MA-L and PS-*b*-Pn(B-*r*-H)MA-H and NMR spectrum for PS-*b*-Pn(B-*r*-H)MA-H. From a sharp peak in the GPC chromatogram, a random copolymer block (Pn(B-*r*-H)MA) was successfully synthesized. From the peak integration in ^{1}H NMR, the composition of PS in the block copolymers was obtained and given in Table 1. Although the exact weight (or volume) fraction of PnBMA in the Pn(B-*r*-H)MA block could not be measured by ^{1}H NMR because of the overlap of the peaks, it could be estimated from DSC results.

Figure 2 gives the DSC thermograms of PnBMA, PnHMA homopolymers, and Pn(B-*r*-H)MA. It is seen that the Pn(B-*r*-H)MA exhibited only a single glass transition (T_g) at 21 °C, which is between that of PnBMA (42 °C) and PnHMA (4 °C). Furthermore, when the Fox equation ($1/T_{g,Pn(B\text{-}r\text{-}H)MA} = w_{PnBMA}/T_{g,PnBMA} + (1 - w_{PnBMA})/T_{g,PnHMA}$, in which w_{PnBMA} is the weight fraction of the PnBMA in the random copolymer) is used, w_{PnBMA} is calculated to be 0.50. This is very similar to the weight fraction of *n*-BMA monomer (0.52) in total feed monomers. The result suggests that the synthesized Pn(B-*r*-H)MA block in this study could be considered as a random copolymer, not a tapered (or gradient) copolymer. This indicates that the reactivities for two monomers are similar because the difference of the number of carbon in the alkyl group between PnBMA ($n = 4$) and PnHMA ($n = 6$) is not large. Figure 3 shows temperature dependences of specific volume (v_{sp}) for PnBMA, PnHMA, and PnPMA homopolymers and Pn(B-*r*-H)MA. It is seen that v_{sp} at a given temperature is monotonically

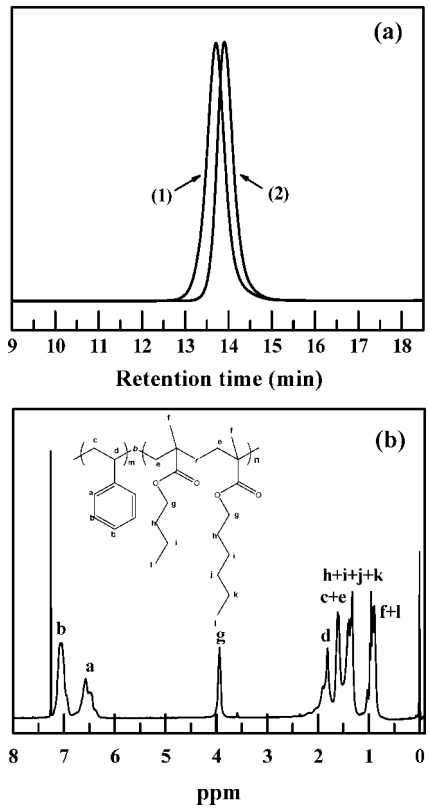

Figure 1. (a) SEC chromatograms of (1) PS-*b*-Pn(B-*r*-H)MA-H and (2) PS-*b*-Pn(B-*r*-H)MA-L. (b) ^{1}H NMR spectrum of PS-*b*-Pn(B-*r*-H)MA-H.

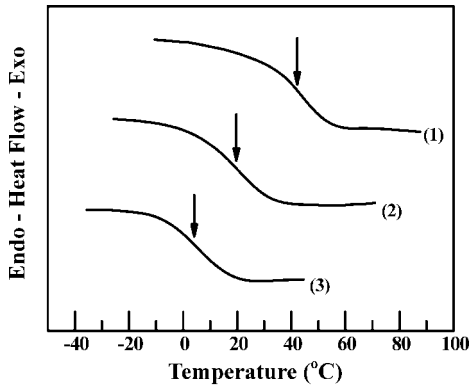

Figure 2. DSC thermograms obtained during the second run with a heating rate of 20 °C/min. T_g of each polymer was marked with an arrow. (1) PnBMA, (2) Pn(B-*r*-H)MA, and (3) PnHMA.

increased with increasing number of *n*. The thermal expansion coefficients (α) obtained above T_g for PnBMA, PnPMA, and PnHMA homopolymers are 6.494×10^{-4}, 6.676×10^{-4}, and 6.989×10^{-4}, respectively. α for Pn(B-*r*-H)MA is 6.842×10^{-4}, which lies in between α of two PnBMA and PnHMA homopolymers and also close to that of PnPMA. The measured thermal expansion coefficients for PnBMA and PnHMA are very similar to those (6.271×10^{-4} for PnBMA and 7.493×10^{-4} for PnHMA) in ref 30.

Figure 4a gives the temperature dependence of the shear modulus (G') of PS-*b*-Pn(B-*r*-H)MA-H and PS-*b*-Pn(B-*r*-H)MA-L. G' of PS-*b*-Pn(B-*r*-H)MA-L decreases gradually with increasing temperature, which is a typical characteristic of homogeneous (or disordered) block copolymers. PS-*b*-Pn(B-*r*-H)MA-H, however, maintained higher G' at higher temperature, indicating that this becomes fully ordered state in the entire

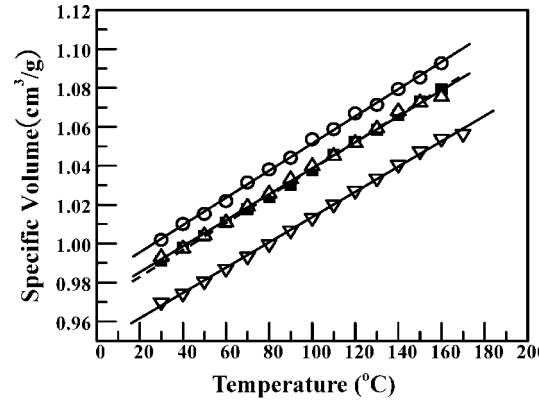

Figure 3. Temperature dependence of specific volume for PnHMA (○), PnPMA (△), and PnBMA (▽) homopolymers (solid lines) and Pn(B-*r*-H)MA (■) (dashed line).

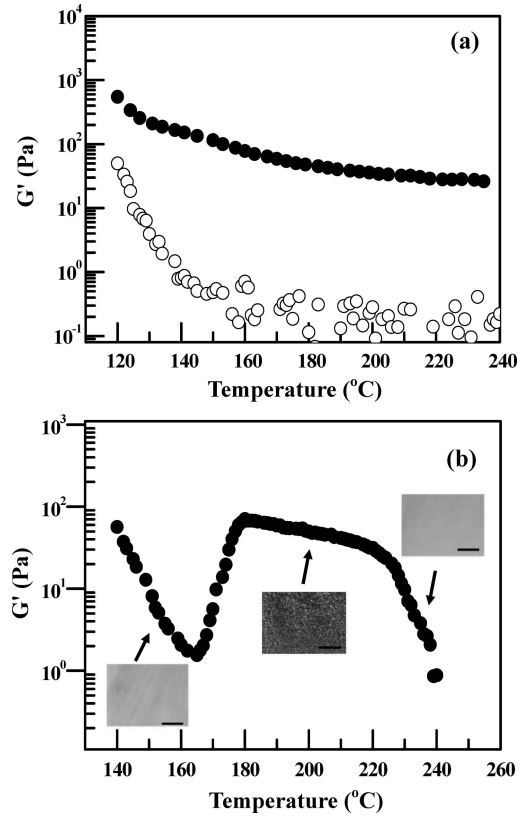

Figure 4. (a) Temperature dependence of G' of PS-*b*-Pn(B-*r*-H)MA-L (○) and PS-*b*-Pn(B-*r*-H)MA-H (●) at $\omega = 0.1$ rad/s and heating rate of 0.5 °C/min. (b) Polarized optical microscopy (POM) images (the scale bar: 10 μm) and temperature dependence of G' for PS-*b*-Pn(B-*r*-H)MA-B3 at $\omega = 0.1$ rad/s and heating rate of 0.5 °C/min.

temperature range. Figure 4b gives POM images of three different temperatures as well as temperature dependence of G' for PS-*b*-Pn(B-*r*-H)MA-B3. The G' decreases rapidly and increases sharply near at 170 °C, which is the LDOT. Then, it dramatically drops as another transition UODT. POM images are consistent with rheological results.

Figure 5a shows SAXS profiles of PS-*b*-Pn(B-*r*-H)MA-B3 at several temperatures. At lower temperatures, a broad peak arising from the correlation hole appears, suggesting that the block copolymer becomes a disordered state. At 178 °C, the first-order peak becomes very sharp, indicating that it is in the ordered state. The higher order peaks, however, did not appear because of the small electron density difference between PS and Pn(B-*r*-H)MA. With further heating, the first-order peak

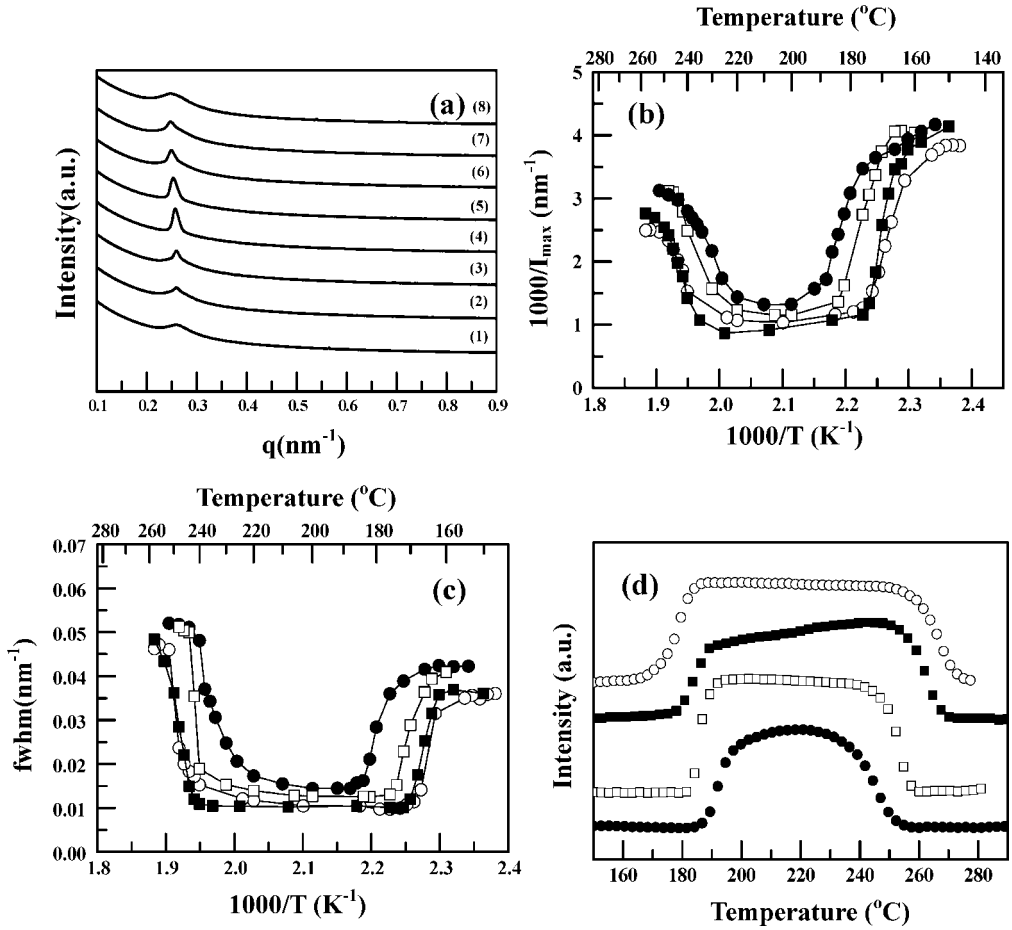

Figure 5. (a) SAXS profiles of PS-*b*-Pn(B-*r*-H)MA-B3 at various temperatures: (1) 170, (2) 174, (3) 178, (4) 200, (5) 220, (6) 234, (7) 238, and (8) 242 °C. (b) Plots of $1/I(q_{max})$ and (c) fwhm vs $1/T$. (d) Temperature dependence of optical birefringence of PS-*b*-Pn(B-*r*-H)MA-B2 (●), PS-*b*-Pn(B-*r*-H)MA-B3 (□), PS-*b*-Pn(B-*r*-H)MA-B4 (■), and PS-*b*-Pn(B-*r*-H)MA-B5 (○).

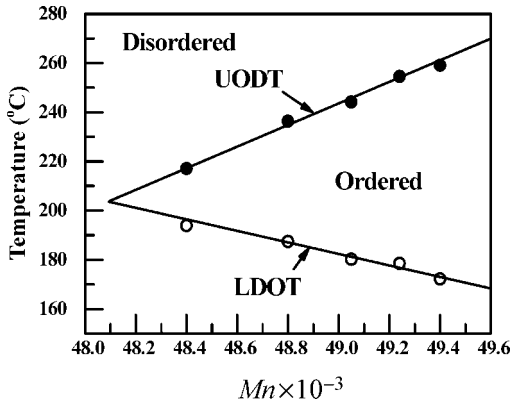

Figure 6. Dependence of LDOT (○) and UODT (●) on M_n.

again becomes broad at 240 °C. From Figure 5a, the LDOT and UODT are 176 and 240 °C. These two temperatures for different PS-*b*-Pn(B-*r*-H)MAs were obtained from plots of the inverse of the SAXS peak intensity and the full width at half-maximum (fwhm) versus the inverse temperature ($1/T$). PS-*b*-Pn(B-*r*-H)MAs having molecular weights between 48 400 and 49 400 exhibited both LDOT and UODT within an experimentally accessible temperature range. These results are also observed from the static birefringence result, as shown in Figure 5d. Figure 6 shows the dependence of LDOT and UODT on M_n. Extrapolation of the data suggests that this block copolymer can be disordered for $M_n < 48\,100$. Previously, we reported that symmetric PS-*b*-PnPMA became disordered for $M_n < 47\,200$.[7]

It is noted that since all the samples employed in this study were prepared by blending of two neat block copolymers (PS-*b*-Pn(B-*r*-H)MA-L and PS-*b*-Pn(B-*r*-H)MA-H), the polydispersity effect of the phase behavior should be considered. Since the weight fraction of PS in the two neat block copolymers is 0.52, the nanostructures of the all blended samples should be lamellae in the ordered state, as stated theoretically[31,32] and experimentally.[33,34] The polydispersity of the blended samples was found to be very similar to that of neat PS-*b*-Pn(B-*r*-H)MA-H. This is because the weight fraction of PS-*b*-Pn(B-*r*-H)MA-H in all samples was 0.75−0.825. The largest polydispersity (which is the case of PS-*b*-Pn(B-*r*-H)MA-B1) was calculated to 1.072, which is quite close to that (1.07) of PS-*b*-Pn(B-*r*-H)MA-H. We further found that GPC chromatogram PS-*b*-Pn(B-*r*-H)MA-B1 did not show bimodal distribution but very similar to that of PS-*b*-Pn(B-*r*-H)MA-H. Therefore, we consider that the transition temperatures of the blended samples are very close to those of the corresponding neat block copolymers at a given total molecular weight.

Figure 7 gives the changes of T_{LDOT} and T_{UODT} for the PS-*b*-Pn(B-*r*-H)MA-B3 with hydrostatic pressure measured by static birefringence. dT_{LDOT}/dP and dT_{UODT}/dP are +595 °C/kbar and −700 °C/kbar, respectively, at pressures above 20 bar. Interestingly, these coefficients are much larger compared with neat PS-*b*-PnBMA ($dT_{LDOT}/dP = +147$ °C/kbar)[25] and PS-*b*-PnHMA ($dT_{ODT}/dP = -60$ °C/kbar)[24] and similar to those for PS-*b*-PnPMA ($dT_{LDOT}/dP = +725$ °C/kbar and $dT_{UODT}/dP = -725$ °C/kbar).[10]

We have suggested theoretically[20,26] and also experimentally[26] that the LDOT type behavior of the homologous series of PS-

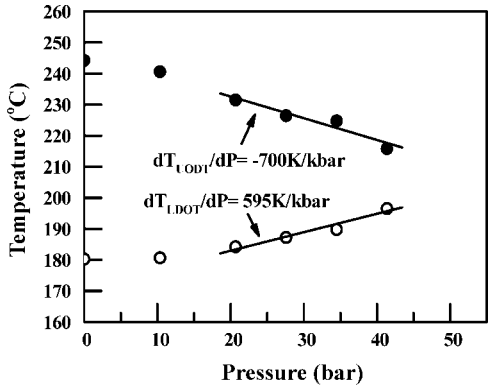

Figure 7. Changes of LDOT (○) and UODT (●) for PS-*b*-Pn(B-*r*-H)MA-B3 with hydrostatic pressure measured by birefringence.

b-poly(*n*-alkyl methacrylates) (PS-*b*-PnAMA) with ethyl (n = 2) to pentyl (n = 5) side group is mainly caused by the temperature change of directional interaction, dipole/induced dipole interaction from the phenyl ring in PS and the polar ester group of PnPMA,[21,22] and the free volume effect. It was also suggested that for PS-*b*-PnHMA (n = 6) a large excluded volume and great flexibility of the hexyl side group hinder this block copolymer from forming the favorable directional interaction, which leads to exhibit only ODT type phase behavior. For this purpose, we introduced the effective Flory interaction parameter χ_F combining two terms (χ_{app} and χ_{comp}). χ_{app} is the dimensionless exchange energy density which is given by $\chi_{app} \propto \Delta\varepsilon/T$. Here, $\Delta\varepsilon$ is the typical exchange energy between like (ε_{ii}) and unlike monomers (ε_{ij}). If there exist directional interactions between unlike monomers, ε_{ij} is modified to be $\varepsilon_{ij} + \delta\varepsilon$ due to the pairwise energy increment.[35] χ_{comp} is expressed as the compressibility (equation-of-state property) difference, which is given by $\chi_{comp} \propto [\partial P/\partial\phi]^2/B_T$, where $\partial P/\partial\phi$ is the derivative of pressure with respect to composition (ϕ) and B_T is the bulk modulus of the copolymer.[36] If $\delta\varepsilon$ is significant as for PS-*b*-PnAMA with $n = 2$ to $n = 5$, $\Delta\varepsilon$ becomes negative at lower temperatures. However, the system entropy hinders such directional interactions at higher temperatures; thus, nondirectional interactions become more important and $\Delta\varepsilon$ becomes positive. Because $\Delta\varepsilon$ in χ_{app} is scaled by the thermal energy kT, χ_{app} starts to decrease beyond a certain temperature, around which χ_{app} reveals a maximum. χ_{comp} is substantial if $\partial P/\partial\phi \neq 0$, but with the increase of temperature the diminished B_T gradually increases χ_{comp}. Therefore, χ_F still possesses a maximum. Such a temperature dependence of χ_F corresponds to the closed-loop type phase behavior. If $\delta\varepsilon$ is insignificant as for PS-*b*-PnHMA, $\Delta\varepsilon$ is insensitive to temperature. In this case, χ_{app} (and also χ_F) decreases with increasing temperature, which is the ODT type phase behavior.

When PnAMA is replaced by a random copolymer consisting of equal amounts of PnBMA and PnHMA, the excluded volume per unit volume becomes roughly similar to that of *n*-pentyl methacrylate, as seen in Figure 3. Also, the large flexibility of the PnHMA is reduced in the average sense due to the random participation of the less flexible PnBMA. Therefore, the average force field (and $\Delta\varepsilon$) generated by the Pn(B-*r*-H)MA block should be similar to that by the PnPMA block. This indicates that when the directional interaction is judiciously controlled by the participating polymer chains, the closed-loop type phase behavior could be observed.

It is also seen in Figure 6 that the size of the loop of PS-*b*-Pn(B-*r*-H)MA is extremely sensitive to M_n, similar to PS-*b*-PnPMA. This result is caused by the flatness of $N\chi_F$ around its maximum, where N is the copolymer chain size (proportional to molecular weight). As $N\chi_F$ is the relevant parameter for the ordering transition, its value is fixed to a certain number at the ODT depending on N. A small change in N thus alters drastically the ordering temperature to have the same $N\chi$ value at ODT.[26,37] It is known that both PS-*b*-PnBMA and PS-*b*-PnHMA are baroplastic.[24−26] They possess a compressibility difference between components as $\partial P/\partial\phi \neq 0$, and thus $\chi_{comp} > 0$. When pressure is increased, the increased B_T reduces χ_{comp} (and therefore χ_F itself), which yields phase mixing upon pressurization. The $\partial P/\partial\phi$ and B_T for PS-*b*-Pn(B-*r*-H)MA might have the averaged values of those for PS-*b*-PnBMA and PS-*b*-PnHMA. The dT/dP of both LDOT and UODT for the PS-*b*-Pn(B-*r*-H)MA is larger than that of either neat PS-*b*-PnBMA or neat PS-*b*-PnHMA.[24−26] The larger dT/dP is attributed to the flatness of $N\chi$ around its maximum, namely, a large change of transition temperature upon pressurization is needed to keep a fixed $N\chi$ value at ODT.[26,37]

Let us provide a more quantitative interpretation for PS-*b*-Pn(B-*r*-H)MA. In our previous publication for the phase behavior of homologous series of PS-*b*-PnAMA, we employed a Hartree (fluctuation correction) analysis based on a compressible random phase approximation (RPA).[24] The required molecular parameters for PS-*b*-PnBMA and PS-*b*-PnHMA are given as follows: for theoretical monomer diameters, $\sigma_{PS} = \sigma_{PnBMA} = 4.04$ and $\sigma_{PnHMA} = 4.12$ Å; for self-interactions, $\varepsilon_{PS}/k = 410.7$, $\varepsilon_{PnBMA}/k = 373.8$, and $\varepsilon_{PnHMA}/k = 354.9$ K; for theoretical chain size N, $(N\pi\sigma^3/6M)_{PS} = 0.418\,57$, $(N\pi\sigma^3/6M)_{PnBMA} = 0.420\,42$, and $(N\pi\sigma^3/6M)_{PnHMA} = 0.437\,71$ cm^3/g. The symbols k and M denote the Boltzmann constant and molecular weight, respectively. As was discussed qualitatively, Pn(B-*r*-H)MA is treated as a pseudo-homopolymer having averaged molecular parameters. From the parameters for PnBMA and PnHMA, we suggest the averaged homopolymer parameters for Pn(B-*r*-H)MA as

$$\varepsilon_{Pn(B\text{-}r\text{-}H)MA} = \varepsilon_{PnBMA}/4 + \varepsilon_{PnHMA}/4 + 2(\varepsilon_{PnBMA}\varepsilon_{PnHMA})^{1/2}/4 \quad (1)$$

$$\sigma_{Pn(B\text{-}r\text{-}H)MA} = (\sigma_{PnBMA} + \sigma_{PnHMA})/2 \quad (2)$$

$$(N\pi\sigma^3/6M)_{Pn(B\text{-}r\text{-}H)MA} = (N\pi\sigma^3/6M)_{PnBMA}/2 + (N\pi\sigma^3/6M)_{PnHMA}/2 \quad (3)$$

Typical Berthelot's rule $(\varepsilon_{PnBMA}\varepsilon_{PnHMA})^{1/2}$ leads to eq 1, where the equal amounts of nBMA and nHMA are mixed to make Pn(B-*r*-H)MA. Equations 2 and 3 are a natural choice for this random copolymer. Evaluating eqs 1−3 yields $\varepsilon_{Pn(B\text{-}r\text{-}H)MA}/k = 364.3$ K, $\sigma_{Pn(B\text{-}r\text{-}H)MA} = 4.08$ Å, and $(N\pi\sigma^3/6M)_{Pn(B\text{-}r\text{-}H)MA} = 0.429\,07$ cm^3/g, which are quite close to those of PnPMA as 368.1 K, 4.04 Å, and 0.430 73 cm^3/g, respectively. The above values of ε_{ii} for different poly(*n*-alkyl methacrylate)s are chosen as $\varepsilon_{PnBMA} > \varepsilon_{PnPMA} > \varepsilon_{Pn(B\text{-}r\text{-}H)MA} > \varepsilon_{PnHMA}$. This is consistent with the experimental results of the magnitude of α for these polymers (see Figure 3), since a polymer with higher ε_{ii} becomes more tightly bound ($\varepsilon_{ii} \propto 1/\alpha$). To give the theoretical monomer diameter for the final PS-*b*-Pn(B-*r*-H)MA system, the Lorentz mixing rule is used as $\sigma = (\sigma_{PS} + \sigma_{Pn(B\text{-}r\text{-}H)MA})/2$, which resolves the discrepancy in monomer diameters. What remains now in performing the calculation is ε_{12} and $\delta\varepsilon$. We do not take any of these parameters as adjustable. When those determined for PS-*b*-PnPMA are adopted here, $\varepsilon_{12}/(\varepsilon_{PS}\varepsilon_{Pn(B\text{-}r\text{-}H)MA})^{1/2} = 0.983$ and $\delta\varepsilon/\varepsilon_{PS} = 0.185$.

We now present the Hartree prediction with the molecular parameters chosen. ODT for symmetric diblock copolymers is determined if $N\chi_F$ evaluated at a wavenumber characterizing their microphases becomes $10.495 + 41.022N^{-1/3}$ regardless of block copolymers having baroplastic or barotropic properties. Figure 8a shows the $N\chi_F$ for the symmetric PS-*b*-Pn(B-*r*-H)MA with two values of M_ns (50 146 (N = 1008) and 49 350 (N =

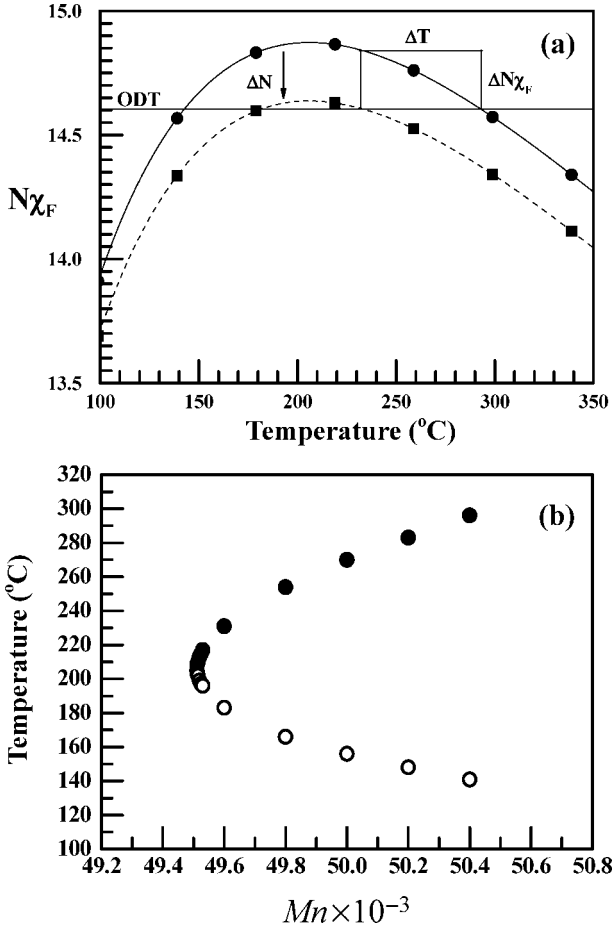

Figure 8. (a) Plot of $N\chi_F$ vs temperature at ambient pressure for the symmetric PS-*b*-Pn(B-*r*-H)MA with two different M_ns (M_n = 50 146 (●) and M_n = 49 350 (■)). The line in plot (a) indicates $N\chi_F$ value at ODT, which should be slightly different for the block copolymers with these two M_ns due to its $N^{-1/3}$ dependence. (b) Plots of the predicted LDOT (○) and UODT (●) vs M_n.

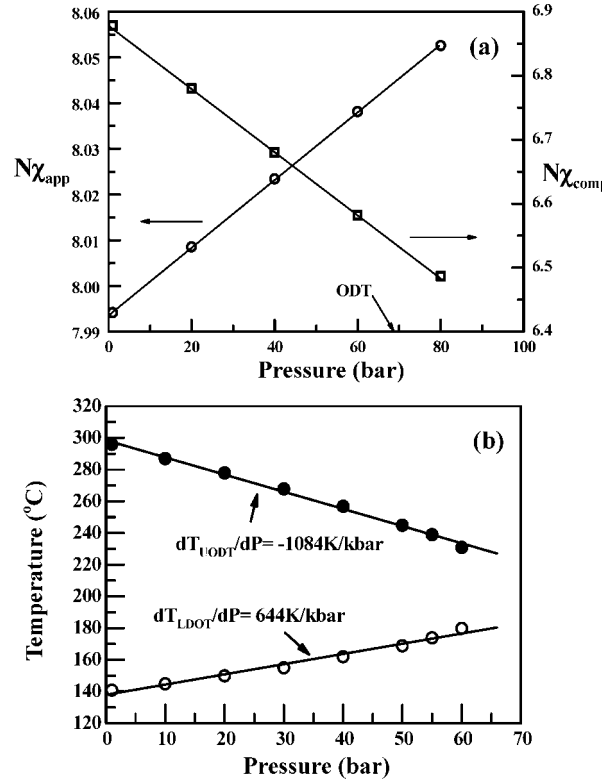

Figure 9. (a) Plot of $N\chi_{app}$ and $N\chi_{comp}$ at 205 °C and (b) plot of predicted LDOT (○) and UODT (●) for PS-*b*-Pn(B-*r*-H)MA with M_n = 50 146 vs hydrostatic pressure.

992)) as a function of temperature. It is seen that $N\chi_F$ at ~205 °C reveals a maximum. The values of $N\chi_{F,ODT}$ for these two M_ns are predicted to be 14.59 and 14.61, respectively. The block copolymer is ordered between LDOT and UODT, where $N\chi_F$ is above $N\chi_{F,ODT}$. As the chain size decreases, $N\chi_F$ decreases by $\Delta N\chi_F$. The new ODT upon the decrease of N should be changed by ΔT. Around the maximum of $N\chi_F$, its slope approaches zero. In this situation, only a slight change in $N\chi_F$ makes enormous changes in ΔT. Such a strong molecular weight dependence of the predicted LDOT and UODT is indeed shown in Figure 8b. Interestingly, the predicted loops depending on M_n are quite close to the experimentally obtained ones. This result, though not perfectly matching, is remarkable since there is no adjustable parameter in estimating the block copolymer phase behavior.

Figure 9a depicts $N\chi_{app}$ and $N\chi_{comp}$ at 205 °C as a function of pressure for PS-*b*-Pn(B-*r*-H)MA of M_n = 50 146. The response of χ_{app} and χ_{comp} to pressure contribute to phase miscibility differently.[19,20,36] The χ_{app}, if $\Delta\varepsilon > 0$, increases upon pressurization because of the increased contact density to hamper miscibility. On the contrary, the applied pressure reduces χ_{comp} to enhance miscibility because of the increased B_T. The overall behavior of $N\chi_{app}$ and $N\chi_{comp}$ reduces $N\chi_F$ upon pressurization because $N\chi_{comp}$ changes more rapidly than $N\chi_{app}$. The closed loop is existent only when $N\chi_F$ is greater than the $N\chi_{F,ODT}$. When pressure becomes 68.3 bar, $N\chi_F$ becomes below the $N\chi_{F,ODT}$, indicating that the closed loop disappears. Figure 9b shows the change of the predicted LDOT and UODT with pressure. Although the predicted pressure coefficients of UODT and LDOT for PS-*b*-Pn(B-*r*-H)MA are somewhat larger than those measured experimentally, these are again remarkable because the prediction was done without using any adjustable parameter. The large pressure coefficients can be understood from the same scheme in Figure 8a. Around the maximum of the $N\chi_F$, a slight reduction in $N\chi_F$ due to pressure makes enormous changes in ΔT.

Before closing this section, we notice two theories to explain the phase behavior PS-*b*-P[nAMA-*r*-n′AMA]) ($n \neq n'$).[38−43] Freed et al. studied with a simplified version of the lattice cluster theory (LCT) the phase behavior of this kind of the block copolymer.[38−41] The detailed structures of monomers with pendant groups were considered as a collection of united atoms, and the associated interactions between those united atoms were also introduced. They explained successfully the observed LDOT behavior of PS-*b*-P(MMA-*r*-LMA) (n = 1 and n' = 12), while both PS-*b*-PMMA and PS-*b*-PLMA only exhibit ODT.[40] The main driving force for ordering in their approach is to resolve the entropic loss in mixing PS and polymethacrylates with different pendant group structures. However, we recently showed that the directional interaction, though weak, between PS and PnAMA with n = 2−5 plays an important role in explaining the LDOT (and closed loop) phase behavior.[21,22] It was further revealed that the PS-*b*-PnAMA with n = 2−4 exhibiting only LDOT inherently possess a loop character with UODT,[14,26] which was not observed in an experimentally accessible temperature range before thermal decomposition. Although above experimental observations are well explained by the molecular model based on the compressible RPA developed by one of us, it would be an interesting subject to predict the closed loop phase behavior in homologous series of PS-*b*-PnAMAs including the present work by using the LCT whose ordering mechanism is totally different from ours.

Meanwhile, Ruzette et al. developed a theory based on a compressible regular solution approach.[42,43] They explained that the observation of LDOT for PS-*b*-P(MMA-*r*-LMA) was attributed to the fact that the specific volume and solubility parameter for P(MMA-*r*-LMA) are similar to those for PnBMA with LDOT. This argument is in one sense consistent with the experimental result, as shown in Figure 3. Namely, the specific volume of Pn(B-*r*-H)MA is similar to that of PnPMA. However, the UODT predicted by this theory for PS-*b*-Pn(B-*r*-H)MA is too high (more than 1000 °C), which is not consistent with the observed closed loop within the experimentally accessible temperatures. Therefore, we consider that the present approach based on the compressible RPA with the directional interaction and free volume should be employed to explain the observed loop phase behavior and pressure coefficients of the transition temperatures of PS-*b*-Pn(B-*r*-H)MA.

4. Conclusions

In this study, we investigated the phase behavior of symmetric PS-*b*-Pn(B-*r*-H)MA with various molecular weights by SAXS, rheometry, POM, and static birefringence. When a random copolymer of Pn(B-*r*-H)MA was used as one of the blocks, PS-*b*-Pn(B-*r*-H)MA showed the closed-loop phase behavior having both LDOT and UODT, which was seen in PS-*b*-PnPMA, when the total molecular weight was judiciously controlled. The phase behavior change by including a random copolymer was predicted by the compressible RPA developed by us.

Acknowledgment. This work was supported by the National Creative Research Initiative Program supported by the Korean Organization of Science and Engineering Foundation (KOSEF). Small-angle X-ray scattering was performed at PLS beamline supported by POSCO and KOSEF. J.C. acknowledges the financial support from the nuclear research program funded by KOSEF and Center for Photofunctional Energy Materials funded by Gyeonggi-do.

References and Notes

(1) Leibler, L. *Macromolecules* **1980**, *13*, 1602.
(2) Bates, F. S.; Fredrickson, G. H. *Annu. Rev. Phys. Chem.* **1990**, *41*, 525.
(3) Fredrickson, G. H.; Bates, F. S. *Annu. Rev. Mater. Sci.* **1996**, *26*, 501.
(4) Hashimoto, T. In *Thermoplastic Elastomers*; Legge, N. R., Holden, G., Schroeder, H. E., Eds.; Hanser: New York, 1987.
(5) Kim, J. K.; Lee, J. I.; Lee, D. H. *Macromol. Res.* **2008**, *16*, 267.
(6) Russell, T. P.; Karis, T. E.; Gallot, Y.; Mayes, A. M. *Nature (London)* **1994**, *368*, 729.
(7) Ryu, D. Y.; Jeong, U.; Kim, J. K.; Russell, T. P. *Nat. Mater.* **2002**, *1*, 114.
(8) Ryu, D. Y.; Park, M. S.; Chae, S. H.; Jang, J.; Kim, J. K.; Russell, T. P. *Macromolecules* **2002**, *35*, 8676.
(9) Ryu, D. Y.; Jeong, U.; Lee, D. H.; Kim, J.; Youn, H. S.; Kim, J. K. *Macromolecules* **2003**, *36*, 2894.
(10) Ryu, D. Y.; Lee, D. J.; Kim, J. K.; Lavery, K. A.; Russell, T. P.; Han, Y. S.; Seong, B. S.; Lee, C. H.; Thiyagarajan, P.*Phys. Rev. Lett.* **2003**, *90*, 235501.
(11) Ryu, D. Y.; Lee, D. H.; Jeong, U.; Yun, S. H.; Park, S.; Kwon, K.; Sohn, B. H.; Chang, T.; Kim, J. K.; Russell, T. P. *Macromolecules* **2004**, *37*, 3717.
(12) Ryu, D. Y.; Lee, D. H.; Jang, J.; Kim, J. K.; Lavery, K. A.; Russell, T. P. *Macromolecules* **2004**, *37*, 5851.
(13) Kim, J. K.; Jang, J.; Lee, D. H.; Ryu, D. Y. *Macromolecules* **2004**, *37*, 8599.
(14) Li, C.; Lee, D. H.; Kim, J. K.; Ryu, D. Y.; Russell, T. P. *Macromolecules* **2006**, *39*, 5926.
(15) Sanchez, I. C.; Panayiotou, C. G. In *Modeling Excess Gibbs Energy in Models for Thermodynamic and Phase Equilibria Calculations*; Sandler, S. I., Ed.; Marcel Dekker: New York, 1994; pp 1−86.
(16) Yeung, C.; Desai, R. C.; Shi, A. C.; Noolandi, J. *Phys. Rev. Lett.* **1994**, *72*, 1834.
(17) Freed, K. F.; Dudowicz, J. *Macromolecules* **1996**, *29*, 625.
(18) Freed, K. F.; Dudowicz, J.; Foreman, K. W. *J. Chem. Phys.* **1998**, *108*, 7881.
(19) Cho, J. *Macromolecules* **2001**, *34*, 1001.
(20) Cho, J. *Macromolecules* **2004**, *37*, 10101.
(21) Kim, H. J.; Kim, S. B.; Kim, J. K.; Jung, Y. M.; Ryu, D. Y.; Lavery, K. A.; Russell, T. P. *Macromolecules* **2006**, *39*, 408.
(22) Kim, H. J.; Kim, S. B.; Kim, J. K.; Jung, Y. M. *J. Phys. Chem. B* **2006**, *110*, 23123.
(23) Ruzette, A. V. G.; Banerjee, P.; Mayes, A. M.; Pollard, M.; Russell, T. P.; Jerome, R.; Slawecki, T.; Hjelm, R.; Thiyagarajan, P. *Macromolecules* **1998**, *31*, 8509.
(24) Ruzette, A. V. G.; Mayes, A. M.; Pollard, M.; Russell, T. P.; Hammouda, B. *Macromolecules* **2003**, *36*, 3351.
(25) Pollard, M.; Russell, T. P.; Ruzette, A.-V.; Mayes, A. M.; Gallot, Y. *Macromolecules* **1998**, *31*, 6493.
(26) Ryu, D. Y.; Shin, C.; Cho, J.; Lee, D. H.; Kim, J. K.; Lavery, K. A.; Russell, T. P. *Macromolecules* **2007**, *40*, 7644.
(27) Balsara, N. P.; Perahia, D.; Safinya, C. R.; Tirrell, M.; Lodge, T. P. *Macromolecules* **1992**, *25*, 3896.
(28) Balsara, N. P.; Dai, H. J.; Kesani, P. K.; Garatz, B. A.; Hammouda, B. *Macromolecules* **1994**, *27*, 7406.
(29) Bolze, J.; Kim, J.; Huang, J.; Rah, S.; Youn, H. S.; Lee, B.; Shin, T. J.; Ree, M. *Macromol. Res.* **2002**, *10*, 2.
(30) Zoller, P.; Walsh, D. J. *Standard Pressure-Volume-Temperature Data for Polymers*; Technomic Pub: Lancaster, 1995; pp 161−164.
(31) Shi, A. C.; Noolandi, J. *Macromolecules* **1995**, *28*, 3103.
(32) Matsen, M. W.; Bates, F. S. *Macromolecules* **1995**, *28*, 7298.
(33) Hashimoto, T.; Yamasaki, K.; Koizumi, S.; Hasegawa, H. *Macromolecules* **1993**, *26*, 2895.
(34) Hashimoto, T.; Koizumi, S.; Hasegawa, H. *Macromolecules* **1994**, *27*, 1562.
(35) In principle, potential directional interactions between the same monomers such as $\pi-\pi$ interactions in PS and C═O dipole interactions in polymethacrylates can be treated in a similar way. However, the given sets of three homopolymer parameters absorb such effects in an average sense, as those parameters are determined from fitting PVT data over a large range of temperature and pressure.
(36) Cho, J. *Polymer* **2007**, *48*, 429.
(37) Li, C.; Li, G. H.; Moon, H. C.; Lee, D. H.; Kim, J. K.; Cho, J. *Macromol. Res.* **2007**, *15*, 656.
(38) Dudowicz, J.; Freed, K. F. *Macromolecules* **1991**, *24*, 5076.
(39) Dudowicz, J.; Freed, K. F. *Macromolecules* **1993**, *26*, 213.
(40) Dudowicz, J.; Freed, K. F. *Macromolecules* **2000**, *33*, 5292.
(41) Freed, K. F.; Dudowicz, J. *Adv. Polym. Sci.* **2005**, *183*, 63.
(42) Ruzette, A.V. G.; Mayes, A. *Macromolecules* **2001**, *34*, 1894.
(43) Ruzette, A.V. G.; Banerjee, P.; Mayes, A. M.; Pollard, M.; Russell, T. P. *J. Chem. Phys.* **2001**, *114*, 8205.

MA800645U